Available online at www.sciencedirect.com
SCIENCE DIRECT
Pattern Recognition 39 (2006) 2101–2114
PATTERN RECOGNITION
THE JOURNAL OF THE PATTERN RECOGNITION SOCIETY
www.elsevier.com/locate/patcog

Fuzzy Cognitive Maps for stereovision matching

Gonzalo Pajares[a,*], Jesús M. de la Cruz[b]

[a]*Dpto. Sistemas Informáticos y Programación, Spain*
[b]*Dpto. Arquitectura de Computadores y Automática, Facultad de Informática.- Universidad Complutense, 28040 Madrid, Spain*

Received 15 July 2005; received in revised form 1 February 2006; accepted 3 April 2006

Abstract

This paper outlines a method for solving the stereovision matching problem using edge segments as the primitives. In stereovision matching the following constraints are commonly used: *epipolar*, *similarity*, *smoothness*, *ordering and uniqueness*. We propose a new matching strategy under a *fuzzy* context in which such constraints are mapped. The fuzzy context integrates both Fuzzy Clustering and Fuzzy Cognitive Maps. With such purpose a network of concepts (nodes) is designed, each concept represents a pair of primitives to be matched. Each concept has associated a fuzzy value which determines the degree of the correspondence. The goal is to achieve high performance in terms of correct matches. The main findings of this paper are reflected in the use of the fuzzy context that allows building the network of concepts where the matching constraints are mapped. Initially, each concept value is loaded via the Fuzzy Clustering and then updated by the Fuzzy Cognitive Maps framework. This updating is achieved through the influence of the remainder neighboring concepts until a good global matching solution is achieved. Under this fuzzy approach we gain quantitative and qualitative matching correspondences. This method works as a relaxation matching approach and its performance is illustrated by comparative analysis against some existing global matching methods.

Keywords: Fuzzy Cognitive Maps; Fuzzy Clustering; Relaxation; Fuzzy; Stereovision; Matching; Similarity; Smoothness; Ordering; Epipolar; Uniqueness

1. Introduction

A major portion of the research efforts of the computer vision community has been directed toward the study of the three-dimensional (3-D) structure of objects using machine analysis of images [1]. We can view the problem of stereo analysis as consisting of the following steps: image acquisition, camera modeling, feature acquisition, image matching, depth determination and interpolation. The key step is that of image matching, that is, the process of identifying the corresponding points in two images that are cast by the same physical point in 3-D space. This paper is devoted solely to this problem.

A correspondence needs to be established between features from two images that correspond to some physical feature in space. Then, provided that the position of centers of projection, the focal length, the orientation of the optical axis, and the sampling interval of each camera are known, the depth can be established by triangulation.

1.1. Constraints applied in stereovision matching

Our stereo correspondence problem can be defined in terms of finding pairs of true matches, namely, pairs of edge segments in two images that are generated by the same physical edge segment in space. These true matches generally satisfy some constraints [2]: (1) *epipolar*, given two segments one in the left image and a second in the right one, if we slide one of them along a parallel direction to the epipolar line, they would intersect (overlap) (Fig. 1); (2) *similarity*, matched edge segments have similar local properties or attributes; (3) *smoothness*, disparity values in a given neighborhood change smoothly, except at a few depth discontinuities; (4) *ordering*, the relative position among two edge-segments in the left image is preserved in the right one for the corresponding matches; (5) *uniqueness*, each

* Corresponding author. Tel.: +34 1 3947546; fax: +34 1 3947529.
E-mail address: pajares@dacya.ucm.es (G. Pajares).

0031-3203/$30.00
doi:10.1016/j.patcog.2006.04.003

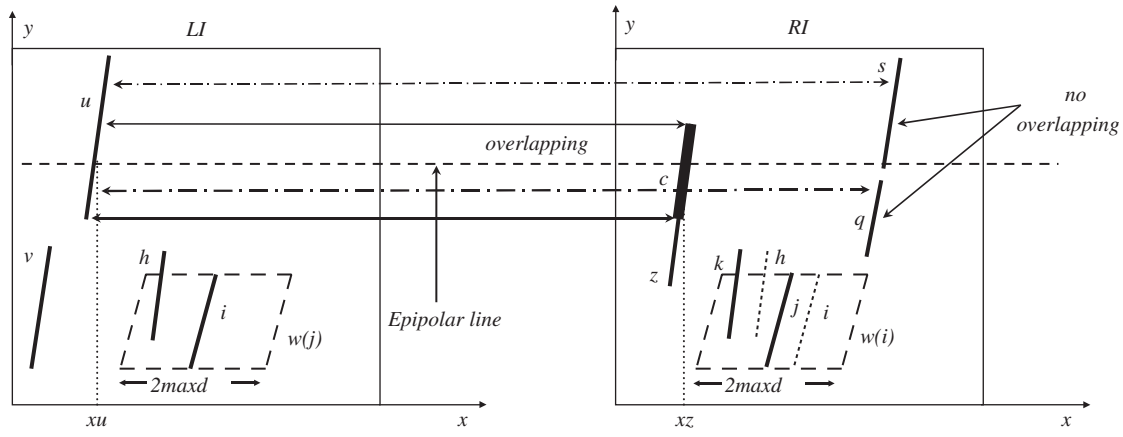

Fig. 1. Overlapping concept, edge-segments interactions and neighborhood for the pair (i, j).

edge-segment in one image should be matched to a unique edge-segment in the other image. The similarity and uniqueness constraints are associated to a *local* matching process, the smoothness and ordering constraints to a *global* matching process and the epipolar is with both, local and global processes. The major difficulty of stereo processing arises due to the need to make *global correspondences*.

1.2. Techniques in stereovision matching

A review of the state-of-art in stereovision matching allows us to distinguish two sorts of techniques broadly used in this discipline: *area-based* and *feature-based*. Area-based stereo techniques use correlation between brightness (intensity) patterns in the local neighborhood of a pixel in one image with brightness patterns in the local neighborhood of the other image [2]. Feature-based methods use sets of pixels with similar attributes, normally, either pixels belonging to edges [3,4], or the corresponding edges themselves [5–13]. We select a feature-based method with edge-segments as features, as they are abundant and commonly used in indoor environments where our mobile robot equipped with the stereovision system navigates. They have been studied in terms of reliability [14] and robustness [15].

We have studied the performance of some local matching strategies: Fuzzy Clustering [12], Support Vector Machines [13], Hebbian learning [16] or a nonparametric probabilistic approach [17]. Nevertheless, we have also verified that the best performance in stereovision matching is achieved under global matching strategies [6–8]. One of the most relevant approaches used for finding the best global matches is relaxation; it refers to a computational mechanism involving unary and binary measurements [18–29] with the purpose of computing and improving any image unit value. Under the stereovision matching framework, the image units are the pairs of features to be matched and the values determine the strength of the correspondences. The unary measurements establish an initial local correspondence by applying local matching constraints. The binary measurements reinforce and weaken the true and false correspondences, respectively by applying global matching constraints through the iterative process involved in the relaxation process.

The following papers use a global relaxation technique based on probabilistic/merit [8,17–25] and optimization through a Hopfield neural network [4,6,28,29].

1.3. Contribution and motivational research

The main contribution of this paper is the combination of two fuzzy approaches: Fuzzy Clustering (FCL) and Fuzzy Cognitive Maps (FCM). This strategy is justified by the following reasons:

(a) The FCL computes the unary measurements through the mapping of the similarity constraint. It has been tested favorably in Ref. [12].
(b) The binary measurements are obtained by considering the consistencies between pairs of features; this can be interpreted as fuzzy causalities in the FCM framework.
(c) The FCM works as a relaxation approach making global correspondences through unary and binary measurements.
(d) The fuzzy causalities are obtained by mapping the global matching constraints, each global constraint generate a kind of fuzzy causality. Different fuzzy causalities can be combined through fuzzy aggregation operators under the fuzzy context.
(e) The updating process is governed by an activation function, which allows to control the convergence as in the well-tested classical original cooperative algorithm proposed by Marr and Poggio [19].
(f) The FCM framework has been studied in terms of stability [30,31].

The results obtained by our FCM relaxation method are similar to the obtained in Ref. [7], as this paper performs

better than other existing strategies, we can conclude that our FCM-based method works appropriately.

The performance for real-time applications is left open for parallel implementations.

Following the FCM framework, each pair of features (edge-segments) to be matched is represented as a concept or node in a network. Each node has associated its own value, which determines the strength of the correspondence. We use the FCL approach for computing the initial matching estimation, i.e. the initial correspondence value for each pair of features. This initial value is updated by the influence of neighboring nodes through the mapping of the stereovision matching (local and global) constraints under the FCM framework. The final correspondences are established based on the final nodes' values. As in Ref. [7], we consider the possible smoothness and ordering constraints violations due to occlusions, camera geometry, objects near the cameras, etc.

1.4. Paper organization

The paper is organized as follows. In Section 2, the full sequential stereovision matching process is described, where the FCL and FCM frameworks are described. The performance of the method is illustrated in Section 3, where a comparative study against other existing global matching methods is carried out. Finally in Section 4 there is a discussion of some related topics.

2. Sequential stereovision matching process

The two cameras have equal focal lengths and are aligned so that their viewing direction is parallel. The plane formed by the viewed point and the two focal points intersects the image plane along a horizontal line known as the epipolar line. A grid pattern of parallel horizontal lines is used for camera alignment. The cameras are adjusted so that the images of these lines coincide. Thus each point in an edge segment lies along the same horizontal (epipolar) line crossing both images. This is part of the system calibration process.

This paper proposes a sequential combination of four methods for solving the stereovision matching problem. Each method is implemented by a module. The system receives as inputs a pair of stereo images left (LI) and right (RI). This pair is processed in order to extract *features and attributes* in the *FAA* module, each pair of extracted features (i, j) is to be matched, the features i and j come from *LI* and *RI*, respectively. For each pair (i, j) an attribute difference vector $\boldsymbol{x}$ is computed. All extracted $\boldsymbol{x}$ vectors are supplied to the *FCL* module, which computes an initial fuzzy concept value C_{ij} for each pair of features, i.e. it computes the unary measurement. This module uses the similarity constraint and requires a previous training process for computing each fuzzy concept value. Until this stage, only a local matching process is carried out. Once all fuzzy matching concept values are obtained, they are supplied to the *FCM* module, which updates each C_{ij} concept value taking into account the weights interconnecting causal concepts. The *FCM* module implements the global matching process. After this stage, perhaps there are still ambiguous matches which are solved by the *unambiguous* (UA) module based on the strength of each state. The output of the system is a set of matches. We give details about the behavior of each module.

2.1. Feature and attribute extraction (FAA)

The contour edges in both images are extracted using the Laplacian of Gaussian filter in accordance with the zero-crossing criterion [32]. For each zero-crossing in a given image, its gradient vector (magnitude and direction) [33,34], Laplacian [34] and variance [35] values are computed from the gray levels of a central pixel and its eight immediate neighbors. Gradient magnitude, Laplacian and variance measure the focusing degree for each zero-crossing [35], i.e. this is a kind of edginess' measurement. The edges are obtained by joining adjacent zero-crossings following the algorithm in Tanaka and Kak [36], where: (1) a margin of deviation of $\pm 20\%$ in gradient magnitude and of $\pm 45°$ in gradient direction is allowed; (2) each detected contour is approximated by a series of piecewise linear line segments [37]. Finally, for every segment, an average value of the four attributes is obtained from all computed values of its zero-crossings. All average attribute values are normalized in the same range.

Each pair of features has two associated 4-dimensional vectors $\boldsymbol{x}_i$ and $\boldsymbol{x}_j$, where the components are the attribute values, and the sub-indices i and j denote features belonging to the left and right images, respectively. A four-dimensional difference measurement vector $\boldsymbol{x}$ is then also obtained from the above $\boldsymbol{x}_i$ and $\boldsymbol{x}_j$ vectors, $\boldsymbol{x}=\boldsymbol{x}_i-\boldsymbol{x}_j=\{x_m, x_d, x_l, x_v\}$. The components of $\boldsymbol{x}$ are the corresponding differences for module and direction gradient, Laplacian and variance values. Only those pairs verifying the following three initial conditions will be processed: (1) their absolute value of the difference in the gradient direction is below a specific threshold, fixed to 25°; (2) their absolute value in the gradient magnitude is also below a fixed threshold, set to 15; and (3) their overlap rate surpasses a certain value, fixed to 0.5. The remaining pairs that do not meet such conditions are directly considered as false correspondences. The overlap is a concept introduced in Medioni and Nevatia [5], two segments u and z overlap if by sliding one of them in a direction parallel to the epipolar line, they would intersect.

Fig. 1 clarifies the overlapping concept. Indeed, segment u in the left image overlaps with segment s in the right image, but segment v does not overlap with s. The overlap rate between edge segments (u, z), α_{uz} is defined as the percentage of coincidence, ranging in [0,1], when two segments u and z overlap, and it is computed taken into account the common overlap length l_c defined by c and the two lengths

for the involved edge segments l_u and l_z, respectively. All lengths are measured in pixels.

$$\alpha_{uz} = 2l_c/(l_u + l_z). \tag{1}$$

Taking into account the above initial conditions (1) and (3) and the parallel optical axis geometry of the stereovision system, we compute the disparity between two edge-segments (u and z in Fig. 1) as follows: trace epipolar lines (four) crossing the common overlapping segment (c), for each line compute x_u and x_z, so the disparity is $(x_u - x_z)$. Then the disparity for edge segments u and z is the averaged disparity for the four pairs of points x_u and x_z.

Fig. 1 also illustrates the neighboring N_{ij} concept between edge-segments (i, j). For each edge segment "i" in the left image we define a window $w(i)$ in the right image and, similarly, for each segment "j" in the right image, we define a window $w(j)$ in the left image. Given the pair (i, j), a new pair (h, k) belongs to N_{ij}, if h lies in $w(j)$ and k lies in $w(i)$. It is said that "a segment h lies in $w(j)$" if at least the 30% of the length of the segment "h" is contained in the $w(j)$ window. The shape of this window is a parallelogram; one side is "i", for left to right match, and the other a horizontal vector of length $2.maxd$. The constant $maxd$ is said the disparity limit, it is set to 15 pixels in this paper and is used for mapping the smoothness constraint as an interconnection value between concepts.

2.2. FCL: A local matching strategy

The stereovision matching problem is viewed as a two classification problem, where a pair of edge-segments is classified as a true or false match (true and false clusters). This method requires a previous training process, where the goal is to obtain the best representative cluster center $\boldsymbol{z}$ for the true matches and the covariance matrix $\boldsymbol{P}$ as a measure of dispersion of the samples around $\boldsymbol{z}$ from the training patterns. These data will be used during the current matching process for computing the initial causal concepts C_{ij} for each pair of edge-segments supplied by the *FAA* module.

1. *Training process*: A detailed description of this process can be found in Ref. [12]; it is based on the observation of a set $X = \{\boldsymbol{x}_1, \boldsymbol{x}_2, \ldots, \boldsymbol{x}_n\}$ of n pattern samples. For each sample $\boldsymbol{x}_i \in X$ compute at the iteration k the membership grade μ_i of such sample with the cluster of true matches and then update the cluster center as follows:

$$\mu_i(k) = \frac{1}{1 + [d_i(k)]^{2/m-1}}, \quad z(k+1) = \frac{\sum_{i=1}^{n} \mu_i^m(k)\boldsymbol{x}_i}{\sum_{i=1}^{n} \mu_i^m(k)}, \tag{2}$$

where $d_i(k)$ is the Mahalanobis distance between the sample $\boldsymbol{x}_i$ and $\boldsymbol{z}$; m is the exponential weight; $\mu_i(k) \in (0, 1]$; the training process stops if $\|\boldsymbol{z}(k+1) - \boldsymbol{z}(k)\| < \varepsilon$ or a number of iterations K is reached; according to the exhaustive results reported in Ref. [12], the following are acceptable values: m=4.2, ε=0.01 and K=10. After the stopping of the training process the covariance matrix is computed as follows:

$$\text{for } i = 1 \text{ to } n \text{ do } \boldsymbol{P}(i+1) = \boldsymbol{P}(i) + \mu_i[(\boldsymbol{x}_i - \boldsymbol{z})^t(\boldsymbol{x}_i - \boldsymbol{z}) - \boldsymbol{P}(i)], \tag{3}$$

where t denotes transpose. Initially $\boldsymbol{z} = \boldsymbol{0}$ (null vector) and $\boldsymbol{P} = \boldsymbol{I}$ (the 4×4 identity matrix).

2. *Local matching process*: Implies the computation of the unary measurement involved in the FCM relaxation process, i.e. the mapping of the similarity matching constraint; given a node (i, j) with a difference vector $\boldsymbol{x}$ the concept value C_{ij} for such node is computed as follows:

$$C_{ij}(\boldsymbol{x}) = \frac{1}{1 + d_M(\boldsymbol{x}, \boldsymbol{z})}, \tag{4}$$

where $d_M(\boldsymbol{x}, \boldsymbol{z}) = (\boldsymbol{x} - \boldsymbol{z})^t \boldsymbol{P}^{-1}(\boldsymbol{x} - \boldsymbol{z})$ is the squared Mahalanobis distance; $C_{ij} \in (0, 1]$.

2.3. FCM: A global matching strategy

The *FCM* module establishes binary measurements by mapping global matching constraints. It receives the network of nodes with each node (concept) initialized according to Eq. (4). As each node represents a pair of features (i, j), under the FCM framework, the value associated to each node can be considered as a concept value for such pair at the time step t, C_{ij}^t, for simplicity we suppress the $\boldsymbol{x}$ difference vector in the left member of the expression (4). From the point of view of the formal theory, the time-varying concept value C_{ij}^t measures the nonnegative occurrence of the fuzzy matching event between pairs of features [38]. The FCM are fuzzy signed directed graphs with feed-back. Each directed edge from causal concept C_{ij}^t to causal concept C_{hk}^t has associated a *causal weight* w_{ij} that measures how much C_{ij}^t causes C_{hk}^t and vice versa, i.e. it is the interconnection weight between two nodes (i, j) and (h, k).

The goal of the FCM process is to increase the consistency of a given pair of edge segments among three constraints (smoothness, ordering and epipolar) so that the concept value of a node representing a correct match can be increased and the concept value of any incorrect match can be decreased during the FCM process [38,39]. Suppose a network with N nodes. Applying the FCM framework the equation for the concept updating is given by Eq. (5)

$$C_{ij}^t = g\left[\sum_{\substack{hk=1 \\ hk \neq ij}}^{N} w_{(ij)(hk)} C_{hk}^{t-1} + w_{(ij)(ij)} C_{ij}^{t-1}\right], \tag{5}$$

where $g(\cdot)$ is the sigmoid activation function of node $(i, j) \equiv ij$. We have defined the sigmoid function by the logistic function [40], i.e. $g(y) = 1/(1 + \exp(-\beta y))$, with the gain β set to 3, the choice of the sigmoid function and the gain setting is motivated by the fact that the causal concept values vary continuously from 0 to 1 and represent the degree of the

matching. So, the output function must cover the continuous range from 0 to 1, moreover in order to avoid severe bias the slope of the sigmoid function must vary smoothly.

In our stereovision matching approach the causal weights are symmetric, i.e. the influence of causal concepts is reciprocal. The self-feedback terms are set to the unity $w_{(ij)(ij)} = 1$, so the previous causal concept contributes as a factor of stabilization during the computation of the current causal concept against an excessive strength coming from the remainder neighboring causal concepts. This is because C_{ij}^{t-1} was initially loaded from the mapping of the strong similarity constraint. The causal weights $w_{(ij)(hk)}$ take values in the fuzzy interval $[-1, +1]$; $w_{(ij)(hk)} = 0$ indicates no causality, $w_{(ij)(hk)} > 0$ indicates causal increase or positive causality: C_{ij}^{t} increases as C_{hk}^{t-1} increases and C_{ij}^{t} decreases as C_{hk}^{t-1} decreases; $w_{(ij)(hk)} < 0$ indicates causal decrease or negative causality: C_{ij}^{t} decreases as C_{hk}^{t-1} increases and C_{ij}^{t} increases as C_{hk}^{t-1} decreases.

The FCM task is to find the most stable network configuration, where the concept values do not change after a number of iterations. Now we map the *smoothness*, *ordering* and *epipolar* stereovision matching constraints under the form of causal weights in order to represent the consistency between the current pair of features under correspondence and the pairs of features in a given neighborhood. The causal weights make global consistency between neighbors pairs of edge segments based on such constraints. Based on Ref. [7] we map the constraints as causal weights as follows.

2.3.1. Mapping the smoothness constraint

The smoothness constraint assumes that neighboring edge segments have similar disparities, except at a few depth discontinuities [5]. Generally, when the smoothness constraint is applied, it is assumed there is a bound on the disparity range allowed for any given segment. This limit is denoted as *maxd*, fixed at 15 pixels in this paper, (see Fig. 1 and discussion in Section 2.1).

Given "*i*" and "*h*" in $w(j)$ and "*j*" and "*k*" in $w(i)$ where "*i*" matches with "*j*" and "*h*" with "*k*" the differential disparity $|d_{ij} - d_{hk}|$, measures how close the disparity between edge segments "*i*" and "*j*" denoted as d_{ij} is to the disparity d_{hk} between edge segments "*h*" and "*k*". The disparity between edge segments is the average of the disparity between the two edge segments along the length they overlap. This differential disparity criterion is used in [4–8,29] among others. We define a compatibility coefficient derived from Refs. [4,7,29] given by

$$c_{(ij)(hk)}(D) = \frac{1}{1 + \exp[\gamma(D/m(D) - 1)]}, \tag{6}$$

where $D = |d_{ij} - d_{hk}|$, $m(D)$ denotes the average of all values D in the pair of stereo images (*LI* and *LR*) under processing. The slope of the compatibility coefficient in Eq. (6) is expressed by γ and varies for each pair of stereo images. To determine γ, it is assumed that the probability distribution function of D is Gaussian with average $m(D)$ and standard deviation $\sigma(D)$, i.e. $p(D) = [1 + \exp[\gamma(D_{(ij)(hk)}/m(D) - 1)]]^{-1}$. Under this assumption and following [41,42], to set the possibility value to 0.1 when the value of cumulative distribution function is 0.9, γ value is calculated by $\gamma = \ln 9((m(D))/(1.282\sigma(D)))$. In our experiments, typical values of γ, $m(D)$ and $\sigma(D)$ are about 6, 9 and 2, respectively. So, values of D near 0 should give high values in the compatibility coefficient $c_{(ij)(hk)}(\cdot) \approx +1$, but near 25 they give low values, $c_{(ij)(hk)}(\cdot) \approx 0$. Note that $c_{(ij)(hk)}(\cdot)$ ranges in (0,1). So, a compatibility coefficient of +1 is obtained for a good consistency between nodes (i, j) and $(h, k)(D = 0)$ and a compatibility of 0 for a bad consistency $(D \gg 0)$. This causal weight embedding the smoothness constraint should indicate positive causality for high compatibility coefficient values and vice versa.

2.3.2. Mapping the ordering constraint

We define the ordering coefficient $O_{(ij)(hk)}$, for the edge-segments according to Eq. (7), which measures the relative average position of edge segments "*i*" and "*h*" in the left image with respect to "*j*" and "*k*" in *RI*, related to the neighboring N_{ij}, it ranges from 0 to 1.

$$O_{(ij)(hk)} = -\frac{1}{S}\sum_{S} o_{(ij)(hk)}$$
$$\text{where } o_{(ij)(hk)} = \|R(x_i - x_h) - R(x_j - x_k)| - 1|$$
$$\text{and} \quad R(r) = \begin{cases} 1 & \text{if } r > 0, \\ 0 & \text{otherwise.} \end{cases} \tag{7}$$

We trace S scanlines (four) along the common overlapping length, each scanline produces a set of four intersection points (i_S and h_S in *LI* and j_S and k_S in the *RI*) with the four edge-segments. Hence, the lower-case o_{ijhk} can be computed as in Ref. [4] considering the above four edge points and it takes 0 and 1 as two discrete values. A value of +1 in the ordering coefficient means that the ordering constraint is preserved. On the contrary, a value of 0 indicates that the ordering constraint is not preserved. The causal weight embedding the ordering constraint should indicate positive causality for a high ordering coefficient value.

2.3.3. Mapping the epipolar constraint (overlapping concept)

The epipolar constraint is mapped through the overlapping concept in Ref. [5], by the overlapping coefficient:

$$\lambda_{(ij)(hk)} = 0.5(\alpha_{ij} + \alpha_{hk}), \tag{8}$$

where α is the overlap rate defined in Eq. (1). Under the epipolar constraint we can assume that correct/incorrect matches should have high/low overlap rates, i.e. the overlapping coefficient should be +1 or 0, respectively and $\lambda_{(ij)(hk)}$ for neighborhoods should be high increasing the consistency. The use of the overlapping criterion is justified by the fact that the edge segments are reconstructed by piecewise linear line segments as described in Section

2.1. The reasoning for the influence of this coefficient in the causal weight is similar to the previous ones for the compatibility and ordering coefficients.

2.3.4. Considering smoothness and ordering constraints violations

There are complex images in which the ordering and smoothness constraints can be violated. In systems with parallel geometry, objects close to the cameras, occlusions and also the definition of a neighborhood (disparity limit) could lead to such violations. So, some excellent neighborhoods could be excluded.

When can we say whether or not there are violations? The ordering constraint is not violated if $O_{(ij)(hk)} > U_0$, with U_0, set to 0.85 in this paper. The smoothness constraint is not violated when: (1) the pairs (i, j) and (h, k) are to be matched, being h a neighborhood of i in $w(j)$ and k a neighborhood of j in $w(i)$, Fig. 1, according to the fixed disparity limit (minimum disparity criterion [5]); (2) the causal concept value at time t, C_{ij}^t has a high positive value although it is not the maximum of all matches (h, k') where h is involved. This is formally expressed as follows: $C_{hk}^t \geqslant H^*(C_{hk'}^t)_{\max} \forall k' \in RI$ with $(C_{hk'}^t)_{\max} = \max\{C_{hk'}^t, \forall k' \in RI\}$, H is set to 0.85 in this paper. The compatibility coefficient is maximum if the matching states are maximum (minimum differential disparity) and vice versa. When no violations occur, the compatibility and ordering coefficients are computed through Eqs. (6) and (7), respectively.

Depending on which of the above conditions is not fulfilled, we say that the ordering, smoothness or both are violated. When this occurs, global consistency is not applicable, and we must fall back on local consistency, i.e. we only consider isolated causal concept values without the neighboring contribution. This is to avoid that true pairs of edge segments are not penalized during the relaxation process due to the violation of such constraints. Depending on which constraint is violated, the corresponding coefficient is,

$$v_{(ij)(hk)} = 0.5(C_{ij}^t + C_{hk}^t), \quad \text{where } v = c, O. \tag{9}$$

2.3.5. Fuzzy criteria for computing the causal weights

Once the smoothness, ordering and epipolar stereovision matching constraints have been mapped, we have available the compatibility, ordering and overlapping coefficients derived from such constraints, respectively. Now the goal is to combine the three coefficients, so that they can be used in the expression (5). Making use of the fuzzy theory, we can consider these coefficients as membership functions, which can be combined in order to compute the causal weight $w_{(ij)(hk)}$. Hence, in our approach the causal weight is considered as a fuzzy measurement (membership value). Under an expert system context [43] is a common practice to use a minimum operator for combining the opinion of several experts. Nevertheless, taking into account the dissertations in Zimmermann [44], a straightforward approach for aggregating fuzzy sets, would be to use the aggregating procedures frequently used in multi-criteria decision theory. They realize the idea of trade-offs between conflicting goals when compensation is allowed, and the resulting trade-offs lie between the most optimistic lower bound and the most pessimistic upper bound, that is, they map between the minimum and the maximum degree of membership of the aggregated sets. Therefore they are called averaging operators. Following the discussion in Ref. [44] about the criteria for selecting appropriate aggregation operators, we find that adaptability is suitable; this can be achieved by parametrization. Thus *min* and *max* operators cannot be adapted at all. They are acceptable in situations in which they fit, by contrast, there are other operators that can be adapted to certain contexts by setting their parameters; we have used the Hamacher's union operator. Taking into account that causal weights are considered as fuzzy membership values and making use of the operator's associativity Eq. (10) is derived. The parameter τ allows a fitting appropriately

$$\mu_{(ij)(hk)} = \frac{(\tau-1)c_{(ij)(hk)}O_{(ij)(hk)} + c_{(ij)(hk)} + O_{(ij)(hk)}}{1 + \tau c_{(ij)(hk)}O_{(ij)(hk)}},$$

$$W_{(ij)(hk)} = \frac{(\tau-1)\mu_{(ij)(hk)}\lambda_{(ij)(hk)} + \mu_{(ij)(hk)} + \lambda_{(ij)(hk)}}{1 + \tau\mu_{(ij)(hk)}\lambda_{(ij)(hk)}}, \tag{10}$$

where $\tau \geqslant -1$, we have found acceptable the behavior of this parameter by setting it to 1. This is because its behavior is a trade-off between maximum and minimum operators [44]. We have tested other values for τ and other parameterized operators (Einstein, Yager, Dubois and Prade among others, Zimmerman) without any apparent improvement in the final results.

As a result of the aggregation's operators, the resulting $W_{(ij)(hk)}$ from Eq. (10) ranges in $[0, +1]$. So, rescaling this interval to $[-1, +1]$, we can derive the final causal weight $w_{(ij)(hk)}$ between features (i, j) and (h, k) as required by Eq. (5). So, we obtain,

$$w_{(ij)(hk)} = 2W_{(ij)(hk)} - 1. \tag{11}$$

So, high coefficient values should give high causal weights i.e. positive causality as expected and vice versa for low coefficient values and negative causality.

2.3.6. Full FCM process

The full FCM process can be summarized as follows:

(1) *Initialization*: Assume a network of N causal concepts or nodes representing pairs of edge segments $(i, j) \equiv ij$. Initially, at $t = 0$, the causal concept values C_{ij}^t are supplied by the FCL module and computed according to Eq. (4).
(2) *FCM process*: Set $t = t + 1$ and $np = 0$; compute the causal weights according to Eq. (11); update each C_{ij}^t according to Eq. (5); if $|C_{ij}^t - C_{ij}^{t-1}| > \varepsilon$ then $np{=}np{+}1$; when all ij nodes are updated, if $np \neq 0$ or $t < t_{max}$ then

start step 2 once again, else stop. Otherwise, the network reaches its stabilization or convergence, i.e. $np = 0$.

(3) *Output*: C_{ij}^t updated.

Where np is the number of nodes for which the matching concept values are modified by the updating procedure, ε is a constant value to accelerate the network stabilization, set to 0.01 in our experiments.

2.3.7. Uniqueness constraint

The *uniqueness* constraint completes the set of matching constraints used for solving our stereovision matching problem.

A left edge segment can be assigned to a unique right edge segment (unambiguous pair) or several right edge segments (ambiguous pairs). The decision about whether a match is correct is made by choosing the greater causal concept value (in the unambiguous case there is only one) whenever it surpasses a previous fixed threshold $U_1(=0.5)$, intermediate value for C_{ij}^t ranging in [0,1]. A true match (i, j) should have $C_{ij}^t = 1$.

The ambiguities produced by broken edge segments are allowed. Hence, it is possible that more than two segments in one image, coming from a broken edge segment, could match with a unique segment in the other image. The following pedagogical example from Fig. 1 clarifies this. The edge segment u in *LI* matches with the broken segment represented by s and q in *RI*, but under the condition that s and q do not overlap, the s and q orientations do not differ by more than $U_2(= \pm 10°)$ and the causal concepts values for both edge segments C_{us}^t and C_{uq}^t are greater than U_1.

After the disambiguation process, the resulting causal concept values determine the degree of matching for each pair of edge-segments.

3. Validation, comparative analysis and performance evaluation

3.1. Design of a test strategy

In order to assess the validity and performance of the proposed method, we have designed the same test strategy used in Ref. [7]. The intention is to compare the performance of the proposed method against the method proposed in such reference and simultaneously against the strategies already used in Ref. [7] for comparative purposes. The testing process is as follows. We have selected 82 stereo pairs of realistic stereo images from an indoor environment. Fig. 2 shows four representative images of this indoor environment; each image is the left image of a stereo pair. All tested images are 512×512 pixels in size, with 256 gray levels. The 82 stereo pairs are classified into three groups: SP1, SP2 and SP3 with 28, 31 and 23 pairs of stereo images, respectively. Each stereo pair consists of two left and right original images and two left and right images of labeled edge segments. Previously, we used an additional set of 15 stereo images to compute the cluster center $\boldsymbol{z}$ and the covariance matrix $\boldsymbol{P}$ according to Eqs. (2) and (3), respectively. Then, after each stereo pair set is processed the true matches are added to the set of training samples for updating $\boldsymbol{z}$ and $\boldsymbol{P}$. The group SP1 consists of stereo images without apparent complexity; Fig. 3 shows a stereo pair representative of the group SP1.

Group SP2 corresponds to scenes where a repetitive structure (vertical books) has been captured; Fig. 4 shows a stereo pair representative of SP2. Finally, group SP3 contains objects close to the cameras, which produce a high range of disparity violating the smoothness and ordering constraints. Fig. 5 is a stereo pair representative of SP3, where we can see the object labeled as 9, 10 in left image and 11, 12 in right image as a characteristic example of an object close to the cameras occluding the edge segment 19 in the right image. Although this last type of images is unusual, its treatment is very important as they could produce fatal errors in navigation systems for example, where the nearest objects must be processed immediately. The SP2 and SP3 are of special interest as they are complex images containing structures that appear with a high degree of difficulty. This kind of images have been studied in depth in Refs. [6,7,13] where similar considerations have been also introduced to deal with the violation of the smoothness and ordering constraints. Therefore, we compare our Fuzzy Cognitive Maps strategy (FCMS) against the Support Simulated Annealing (SANN) in Ref. [7], but also with the method described in Ref. [8] which is a Relaxation Labeling (RELB) approach and the method described in Ref. [6], which is an optimization approach based on the Hopfield Neural Network (HNNB1). FCMS and SANN use the same philosophy: (a) both map the similarity constraint through a local matching strategy, Fuzzy Clustering and Support Vector Machines, respectively; (b) they map the same set of global matching constraints through the FCM and Simulated Annealing relaxation processes, respectively.

Both, RELB and HNNB1 apply the similarity constraint by computing a matching probability based on the estimation of a probability density function through the Bayes's theory. The matching probabilities are used as the inputs for the relaxation and optimization processes, respectively. From these processes, RELB performs an iteration procedure by applying smoothness, ordering and uniqueness constraints. HNNB1 performs the optimization process by mapping the smoothness and uniqueness in an energy function which is to be minimized. From HNNB1, we have implemented a new version HNNB2, by mapping the ordering constraint as an energy function to be minimized and applying the similarity constraint as the 4-dimensional difference null vector $\boldsymbol{x}$. HNNB2 can be considered a very close approach to that described in Ref. [4], although this work uses edge pixels as features, we have modified the original method in Ref. [4] to use edge-segments as in SANN. Also, from HNNB1 we have implemented a new version, HNNP, where the similarity constraint is mapped by estimating a probability density function through the Parzen's window [17].

Fig. 2. Left stereo images representative of the indoor environment.

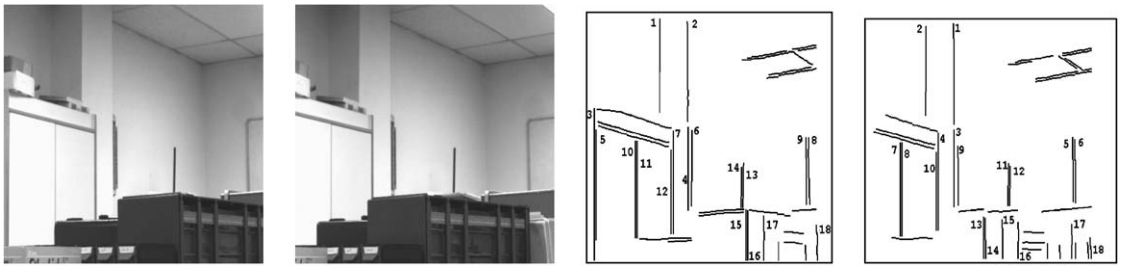

Fig. 3. Group SP1 (a) and (b) original left and right stereo images; (c) and (d) labeled edge segments in left and right images.

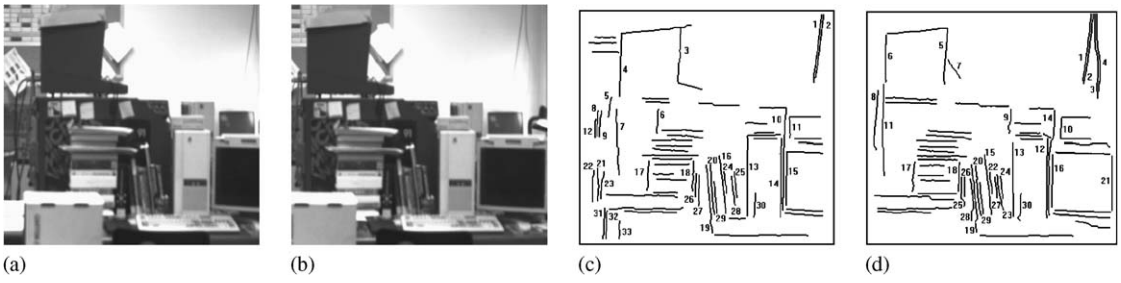

Fig. 4. Group SP2 (a) and (b) original left and right stereo images; (c) and (d) labeled edge segments in left and right images.

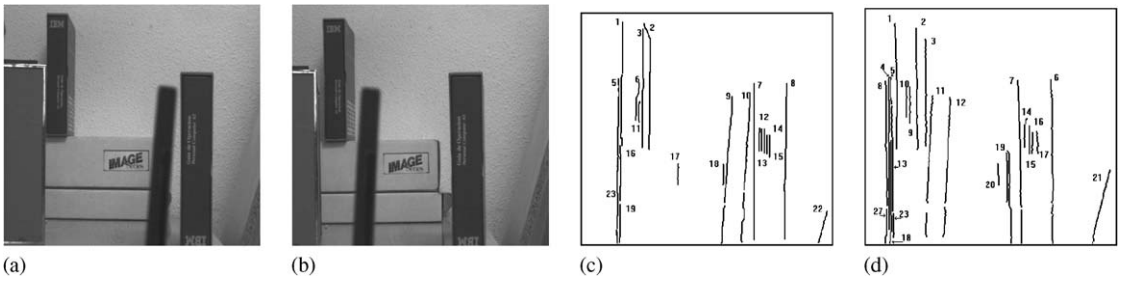

Fig. 5. Group SP3 (a) and (b) original left and right stereo images; (c) and (d) labeled edge segments in left and right images.

We have also compared our approach with the Stochastic Stereovision Matching Method (SSVM) in Ref. [41], also used in Ref. [42]. This method uses the regularization criterion proposed in Ref. [45], where an energy functional is minimized based on a penalty functional which measures the dissimilarity between corresponding features (similarity constraint) and a stabilizing functional by which the smoothness constraint is imposed. The energy minimization is carried out through the Simulated Annealing algorithm, we have used a value of 50 as in Ref. [41] for the regularization parameter λ (this works well for images quantized in 8-bit values) and the same neighborhood criteria as that used in this paper. Two differences are considered in this implementation with respect to our implementation: (1) the edge-segments disparities are the outputs obtained in SSVM, which are used to obtain the correspondences and (2) the

hierarchical coarse-to-fine control structure with re-heating in Ref. [42] is not used in our implementation.

Finally we have chosen the minimum differential disparity algorithm (MDDA) [5] for comparative purposes for the following reasons: (1) it is a merit relaxation approach; (2) it applies the commonly used constraints (similarity, smoothness and uniqueness); (3) it uses edge segments as features and the contrast and orientation of the features as attributes; and (4) some concepts of MDDA, such as minimum differential disparity, overlapping concept, disparity limit or average disparity are used in our FCMS approach. Table 1 summarizes the main differences between the eight strategies compared. All methods use edge-segments as features and the same four attributes.

We have used the same set of training patterns for estimating z and $\boldsymbol{P}$ in FCMS and a decision function in SVSA and also the probabilities densities in RELB, HNNB1 and HNNB2. Once each set SP1, SP2 and SP3 is processed, we use the true matches as new training patterns, which are added to the old ones, for new estimations.

3.2. Comparative analysis

The system processes the SP1, SP2 and SP3 groups. Of all the possible combinations of pairs of matches formed by segments of left and right images only 643, 584 and 474 pairs are considered for SP1, SP2 and SP3, respectively under the thresholds and settings given in Section 2.1. The computed results with the thresholds and settings given in Section 2.1 are summarized in Table 2. It shows the percentage of successes for each group (SP1, SP2 and SP3) and for each method (FCMS, SANN, RELB, HNNB1, HNNB2, HNNP, SSVM, and MDDA) as a function of the number of iterations. Iteration 0 corresponds to the results for the local matching process, Fuzzy Clustering and Support Vector Machines in FCMS and SANN, respectively. This is the starting point for the FCM process in our approach, Section 2.3.6.

Decision process: When the network stabilization has been achieved or the maximum number of iterations ($t_{max} = 100$) reached, there are still both unambiguous pairs of segments and ambiguous ones, depending on either one, and only one, or several right image segments corresponding to a given left image segment. In any case, the decision about whether a match is correct or not is made by choosing the result of greater causal concept value in FCMS, greater state value in SANN, greater probability in RELB, HNNB1, HNNB2 and HNNP, and the best merit value for MDDA.

In the unambiguous case there is only one. The values must be greater than the corresponding intermediate value: 0.5 for the probabilities in RELB, HNNB1, HNNB2 and HNNP, 0 for the states in SANN and 0.5 for the causal concept values in FCMS.

According to values from Table 2, the following conclusions may be inferred:

(1) *Local matching process* (iteration 0, still the iteration processes have not been triggered): The best performances are achieved with FCMS and SANN. This means that the FCL and the Support Vector Machines appear as good local matching methods. The results obtained by HNNP are also good. The methods without estimation (HNNB2 and MDDA) obtain the worst results at this phase.

(2) *Global matching process Group SP1*: The best performance is achieved with FCMS. The local matching results are improved through the global matching process. The ordering constraint is not decisive: HNNB2 (with ordering) obtains worse results than HNNB1 and HNNP (without ordering). There are no violations in the smoothness and ordering constraints. In Ref. [7] is reported that SANN reaches its equilibrium with an average of 65 iterations, with such number of iterations the performance of SANN is comparable to the performance of FCMS with 35 iterations. As this assertion is also valid for groups SP1 and SP2, we can conclude that the fuzzy causal approach under FCMs is suitable in terms of performance in stereovision matching, i.e. the causal reasoning and decision process under a fuzzy point of view is consistent with that of the human. This is the reason for the better performance of our FCMS approach against the remainder methods, particularly against the SANN approach. Another important reason comes from Eq. (5), where the previous causal concept C_{ij}^{t-1} contributes to the updating of C_{ij}^{t}, this implies that the network achieves a rapid stabilization because we are starting from the initial values loaded through the Fuzzy Clustering approach, that applies the strong similarity constraint. Finally, SANN only reaches the 96.0 in percentage with 400 iterations, as reported in Ref. [41]. MDDA obtains the worst results.

Group SP2 (containing repetitive structures): FCMS achieves the best results under the fuzzy consideration. The ordering constraint, once again, is not relevant (HNNP achieves better results than RELB). The consideration of the smoothness constraint violation is decisive (HNNB2 achieves poor results as compared to FCMS, SANN, RELB, HNNB1 or HNNB2) and the ordering constraint violation has low relevance (HNNP obtains better results than RELB). The behavior of SSVM is similar to that of group SP1. MDDA obtains the worst results.

Group SP3 (structures violating the smoothness and ordering constraints): The best performance is achieved once again with FCMS. As expected, the methods that take into account the smoothness and the ordering violation (FCMS, SANN and RELB) achieve better results than HNNB1 and HNNP (only smoothness) and of course better than HNNB2 or SSVM (without any consideration). The results obtained with the MDDA decrease as the number of iterations increases, because the merit of false matches increases (pairs (3,3) or (2,2) in Fig. 5).

3.3. Experimental results and thresholds settings

Table 3 summarizes the set of thresholds and settings with a description, their values (used in this paper for obtaining

Table 1
Summary of stereovision matching methods and constraints

	Stereovision matching constraints					Constraints violation	
	Similarity	Smoothness	Ordering	Epipolar	Uniqueness	Smoothness	Ordering
FCMS	Fuzzy clustering	Mapped as coefficients aggregated in the causal weight between concepts	Mapped as coefficients aggregated in the causal weight between concepts	Mapped as coefficients aggregated in the causal weight between concepts	Applied by selecting the highest causal concept values	Yes	Yes
SVSA	Support Vector Machines	Mapped as an energy minimized by Simulated Annealing	Mapped as an energy minimized by Simulated Annealing	Mapped as an energy minimized by Simulated Annealing	Applied by selecting the highest state values	Yes	Yes
RELB	Bayes probability density estimation	Probabilistic relaxation	Probabilistic relaxation	Mapped under the overlapping concept	Applied by selecting the highest probabilities	Yes	Yes
HNNB1	Bayes probability density estimation	Mapped as an energy minimized by Hopfield	No	Mapped under the overlapping concept	Mapped as an energy minimized by Hopfield	Yes	No
HNNB2	Euclidean distance without estimation	Mapped as an energy minimized by Hopfield	Mapped as an energy minimized by Hopfield	Mapped under the overlapping concept	Mapped as an energy minimized by Hopfield	No	No
HNNP	Parzen's window probability density estimation	Mapped as an energy minimized by Hopfield	No	Mapped under the overlapping concept	Mapped as an energy minimized by Hopfield	Yes	No
SSVM	Mapped as an energy minimized by regularization	Mapped as an energy minimized by regularization	No	Implicit application by image registration	No	No	No
MDDA	Qualitative Boolean function	Merit function relaxation	No	Implicit application by image registration	Applied by selecting the highest merits	No	No

Table 2
Percentage of successes for the groups of stereo-pairs SP1, SP2 and SP3

Iteration #	0			15			35		
SP#	SP1	SP2	SP3	SP1	SP2	SP3	SP1	SP2	SP3
FCMS	84.2	66.9	79.2	87.8	81.7	84.8	96.1	93.2	94.6
SANN	83.9	67.6	78.3	85.2	78.3	81.2	93.6	91.2	92.5
RELB	77.1	65.9	62.6	81.3	78.4	81.9	91.3	89.7	90.7
HNNB1	77.1	65.9	62.6	80.9	76.1	80.5	90.1	89.7	92.2
HNNB2	73.1	58.5	57.8	79.1	66.5	63.2	88.5	70.1	67.5
HNNP	82.0	67.6	66.3	82.2	81.0	86.3	93.9	91.0	92.4
SSVM	0	0	0	64.5	53.1	36.2	76.2	75.9	56.3
MDDA	72.1	57.1	56.9	77.1	66.5	58.8	83.3	74.2	57.1

the above results), relevance (high, medium or low) and comments.

In Ref. [7] are reported some experiments and conclusions for determining the influence of the thresholds involved in FAA, UA; in Ref. [12] we also give details about the parameters involved in the FCL. Hence, the FCMS approach can be easily reproduced.

The parameters involved in the FCM process are well controlled even if those with high relevance. Hence, we can conclude that our FCMS approach can be easily reproduced.

3.4. Time complexity analysis

Table 4 summarizes the results in terms of time complexity for the full process (FAA, FCM and UA). The analysis is carried out for each group of stereo pairs, first column; the number of stereo images for each group is displayed in the second column; the number of pairs of features (edge-segments) for each group is shown in the third column; the average number of pairs of edge segments for each pair of stereo images is displayed in the fourth column; the average execution time in seconds for each stereo image pair is shown in fifth, sixth and seventh columns for FAA, FCM and UA processes, respectively. The time for FCM is computed after the execution of 35 iterations according to the results in Table 2.

The execution times have been obtained from a code implemented in MATLAB and then compiled under Microsoft Visual C++ and executed on a Pentium IV at 2.5 GHz with 1 GB RAM. From results in Table 4 we can conclude that the time is directly proportional to the number of pairs of edge segments processed. We also can see that an important time is spent during the FAA process. Moreover, as already reported in the literature relaxation approaches are computational intensive. For real time applications or critical time scheduling, it is suggested the implementation under parallel architectures. So, during the FAA process each image of the stereo pair can be processed in different processors and then the FCM iterative process could be separated into different clusters of nodes and those clusters assigned to different processors. Also, we can point out that the execution times for other global matching strategies analyzed fall in similar ranges.

3.5. Extensions

The FCM relaxation scheme can be applied to different stereovision matching schemes involving different features, such as edge-pixels, corner-pixels, curved segments or regions, by modifying or fitting the unary and binary relations. This implies that the unique requirement is the appropriated mapping of the local stereovision matching constraints for unary and the global stereovision matching constraints for binary. Taking into account Eq. (5) , the concept values C_{ij} and the causal weights w_{ij} are obtained from the unary and binary measurements, respectively. If several unary or binary measurements are obtained, we can apply the Hamacher's union operator as in Eq. (10). In our approach this operator is used only for combining the three binary measures used. The relaxation process is applied as in this approach. Some examples for computing the unary and binary measurements are given below:

(a) *Curve-segments*: In Nasrabadi [22] curved-segments are extracted by joining zero-crossings according to the procedure described in Ballard [46]. Each curved-segment is labeled and its centroid computed. The unary is a measure of local similarity computed as a ratio between the Hough accumulator value obtained from the comparison between the left and right R-tables of the involved curved-segment. The binary relation is a compatibility measure computed from the distances between the four centroids involved. The concept values and causal weights required by our FCM approach can be directly obtained from the corresponding measurements. Shan and Zhang [25] compute the unary measurement by selecting seed points on both the left and the right curves, the right seed points are obtained by intersecting the epipolar lines of the left seed points with the curve in the right image; for each seed point on the left curve and its corresponding point in the right curve a correlation score between their neighborhoods is computed. This correlation score should be the concept value in our FCM approach. The binary measurement in Ref. [25] is obtained as a weighted

Table 3
Thresholds and settings used in this paper

Module	Description	Value (s)	Relevance	Comments
FAA	Gradient edge pixel joining (magnitude, direction)	±20%, ±45°	Low	Could range in ±30% and ±90°
	Gradient edge segment difference for matching (magnitude, direction)	15, 25°	Medium	Could range between [0,30] and [0°, 45°], respectively. If the values increase, the number of pairs to be matched increases
	Overlap rate	0.5	Medium	Ranges in [0,1]. High values decreases the number of pairs and do not allow broken edge segments
	m, ε and K (Section 2.2, training process)	4.2, 0.01, 10	Low	m could range in [3.5, 5.2]; ε and K could reach 0.1 and 30, respectively
FCM	Disparity limit, *maxd*	15	High	Depends on the baseline in the optics system geometry. In our system the baseline is 20 cm. Could range in [5,25]
	Determines the neighborhood			
	Compatibility coefficient slope, γ in Eq. (6)	6	High	Derived from Refs. [41,42]. Could range in [2,15]
	Constraint violations, U_0, H	0.85	Medium	High values are required for causal concepts of matched edge segments
	Parameter in the Hamacher's operator, τ	1	Low	Compensation parameter between optimistic and pessimistic bounds for aggregation fuzzy sets. $\tau \geqslant -1$
	Sigmoid function parameter, β	3.0	Low	Well tested in the neural network context
	Maximum number of iterations, t_{max}	100	High	Must be sufficient to ensure the convergence, greater than 35
UA	Disambiguation, U_1	0.5	Low	This is the intermediatestate value. It ranges in $[-1, 1]$
	Difference in segments orientations, U_2	±10°	Low	The system geometry limits such difference. It could reach ±20°

Table 4
Time complexity analysis

SP#	Number of pairs of stereo images	Number of pairs of edge segments	Average number of pairs of edge segments for stereo image pair	Average time for each stereo image pair in seconds		
				FAA	FCM 35 iterations	UA
SP1	28	643	23.0	3.2	4.2	0.06
SP2	31	584	18.8	2.6	3.5	0.05
SP3	23	474	20.6	2.9	3.7	0.04

combination of K 4-dimensional random vectors. A curve is approximated by K line segments, each line segment is connected by two seed points. The four components of each 4-dimensional vector are obtained by subtracting the x–y positions for the seed points in the left image and their homologues in the right one. The homologues are obtained by applying a transformation (rotation and translation) to each line segment in the left image. Applying our FCM approach these K measurements could be combined through the Hamacher's operator and the causal weight obtained.

(b) *Edge-pixels or corners*: In Do et al. [26] the unary measurement is obtained from the similarity constraint, the causal concept is inversely proportional to the local intensity difference between a pair of edge-pixels in both images. A compatibility coefficient is calculated by applying the smoothness constraint, this should be the causal concept in our FCM approach. In Ref. [4] the unary and binary measurements are computed under a similar criterion that the used in our proposed FCM method.

(c) *Regions*: Marapane and Trivedi [47] use mean gray level, area, perimeter, width, length and aspect ratio as attributes for each region. From these attributes, we can compute a difference vector in a similar fashion that described in Section 2.1, i.e. a unary measurement. The binary measurements could be derived from the compatibilities established in Lopez and Pla [48].

4. Concluding remarks

The stereo correspondence problem is formulated as two local and global matching fuzzy processes through the FCL and the FCM strategies, respectively. As already reported, a global process after a local one improves always the results substantially. In global strategies, the consideration of the smoothness and ordering violations also improves the results when violations occur. The proposed FCMS approach performs better, including violations, than the remainder methods and requires less number of iterations than other techniques (SANN) to achieve identical performances. The setting of the parameter's values involved has proven to be acceptable. Its performance is verified against some existing matching strategies. The FCMS method can be applied to other matching strategies involving different types of features. Hence, the proposed method under the fuzzy context is a suitable approach for solving the stereovision matching problem. As reported in the literature any sequential implementation of relaxation approaches is computational intensive. It should be suitable its execution under a parallel architecture.

Acknowledgments

Part of the work has been performed under Projects CICYT DPI2002-02924 and CICYT TAP94-0832-C02-01. The authors wish to acknowledge the constructive recommendations provided by the reviewers.

References

[1] D. Scharstein, R. Szeliski, A taxonomy and evaluation of dense two-frame stereo correspondence algorithms, Int. J. Comput. Vision 47 (1/2/3) (2002) 7–42.
[2] L. Tang, C. Wu, Z. Chen, Image dense matching based on region growth with adaptive window, Pattern Recognition Lett. 23 (2002) 1169–1178.
[3] W.E.L. Grimson, Computational experiments with a feature-based stereo algorithm, IEEE Trans. Pattern Anal. Mach. Intell. 7 (1985) 17–34.
[4] Y. Ruichek, J.G. Postaire, A neural network algorithm for 3-D reconstruction from stereo pairs of linear images, Pattern Recognition Lett. 17 (1996) 387–398.
[5] G. Medioni, R. Nevatia, Segment based stereo matching, Comput. Vision Graphics Image Process. 31 (1985) 2–18.
[6] G. Pajares, J.M. Cruz, J. Aranda, Relaxation by Hopfield network in stereo image matching, Pattern Recognition 31 (5) (1998) 561–574.
[7] G. Pajares, J.M. Cruz, On combining support vector machines and simulated annealing in stereovision matching, IEEE Trans. Syst. Man Cybern. Part B 34 (4) (2004) 1646–1657.
[8] G. Pajares, J.M. Cruz, J.A. López-Orozco, Relaxation labeling in stereo image matching, Pattern Recognition 33 (2000) 53–68.
[9] J.P. Starink, E. Backer, Finding point correspondences using simulated annealing, Pattern Recognition 28 (2) (1995) 231–240.
[10] J.M.M. Montiel, D. Orth, Indoor robot motion based on monocular images, Robotica 19 (2001) 331–342.
[11] A. Luo, W. Tao, H. Burkhardt, A new multilevel line-based stereo vision algorithm based on fuzzy techniques, in: Proceedings of the 13th International Conference on Pattern Recognition, vol. 1 (25–29), 1996, pp. 383–387.
[12] G. Pajares, J.M. Cruz, A new learning strategy for stereo matching derived from a fuzzy clustering method, Fuzzy Sets Syst. 110 (3) (2000) 413–427.
[13] G. Pajares, J.M. Cruz, Stereovision matching through support vector machines, Pattern Recognition Lett. 24 (15) (2003) 2575–2583.

[14] D.H. Kim, R.H. Park, Analysis of quantization error in line-based stereo matching, Pattern Recognition 8 (1994) 913–924.
[15] D.M. Wuescher, K.L. Boyer, Robust contour decomposition using a constraint curvature criterion, IEEE Trans. Pattern Anal. Mach. Intell. 13 (1) (1991) 41–51.
[16] G. Pajares, J.M. Cruz, Stereo matching using Hebbian learning, IEEE Trans. Syst. Man Cybern. Part B: Cybern. 29 (4) (1999) 553–559.
[17] G. Pajares, J.M. Cruz, The non-parametric Parzen's window in stereovision matching, IEEE Trans. Syst. Man Cybern. Part B: Cybern. 32 (2) (2002) 225–230.
[18] R. Hummel, S. Zucker, On the foundations of relaxation labelling processes, IEEE Trans. Pattern Anal. Mach. Intell. 5 (1983) 267–287.
[19] D. Marr, T. Poggio, A computational theory of human stereovision, Proc. R. Soc. London B 207 (1979) 301–328.
[20] K.P. Han, T.M. Bae, Y.H. Ha, Hybrid stereo matching with a new relaxation scheme of preserving disparity discontinuity, Pattern Recognition 33 (2000) 767–785.
[21] A. Rosenfeld, R. Hummel, S. Zucker, Scene labelling by relaxation operation, IEEE Trans. Syst. Man Cybern. 6 (1976) 420–453.
[22] N.M. Nasrabadi, A stereo vision technique using curve-segments and relaxation matching, IEEE Trans. Pattern Anal. Mach. Intell. 14 (5) (1992) 566–572.
[23] K.E. Price, Relaxation matching techniques—a comparison, IEEE Trans. Pattern Anal. Mach. Intell. 7 (5) (1985) 617–623.
[24] W.J. Christmas, J. Kittler, M. Petrou, Structural matching in computer vision using probabilistic relaxation, IEEE Trans. Pattern Anal. Mach. Intell. 17 (8) (1995) 749–764.
[25] Y. Shan, Z. Zhang, New measurements and corner-guidance for curve matching with probabilistic relaxation, Int. J. Comput. Vision 46 (2) (2002) 157–171.
[26] K.H. Do, Y.S. Kim, T.U. Uam, Y.H. Ha, Iterative relaxational stereo matching based on adaptive support between disparities, Pattern Recognition 31 (8) (1998) 1049–1059.
[27] K.P. Han, T.M. Bae, Y.H. Ha, Hybrid stereo matching with a new relaxation scheme of preserving disparity discontinuity, Pattern Recognition 33 (2000) 767–785.
[28] M.S. Mousavi, R.J. Schalkoff, ANN implementation of stereo vision using a multi-layer feedback architecture, IEEE Trans. Syst. Man Cybern. 24 (8) (1994) 1220–1238.
[29] N.M. Nasrabadi, C.Y. Choo, Hopfield network for stereovision correspondence, IEEE Trans. Neural Networks 3 (1992) 123–135.
[30] Q. Cheng, Z.T. Fang, The stability problem for fuzzy bidirectional associative memories, Fuzzy Sets Syst. 132 (2002) 83–90.
[31] A.S. Martchenko, I.L. Ermolov, P.P. Groumpos, J.V. Poduraev, C.D. Stylios, Investigating stability analysis issues for fuzzy cognitive maps, 11th Mediterranean Conference on Control and Automation, 2003, pp. 1–6 (CD-ROM).
[32] A. Huertas, G. Medioni, Detection of intensity changes with subpixel accuracy using Laplacian–Gaussian masks, IEEE Trans. Pattern Anal. Mach. Intell. 8 (5) (1986) 651–664.
[33] J.G. Leu, H.L. Yau, Detecting the dislocations in metal crystals from microscopic images, Pattern Recognition 24 (1991) 41–56.
[34] M.S. Lew, T.S. Huang, K. Wong, Learning and feature selection in stereo matching, IEEE Trans. Pattern Anal. Mach. Intell. 16 (9) (1994) 869–881.
[35] E.P. Krotkov, Active Computer Vision by Cooperative Focus and Stereo, Springer, New York, 1989.
[36] S. Tanaka, A.C. Kak, A rule-based approach to binocular stereopsis, in: R.C. Jain, A.K. Jain (Eds.), Analysis and Interpretation of Range Images, Springer, Berlin, 1990, pp. 33–139.
[37] R. Nevatia, K.R. Babu, Linear feature extraction and description, Comput. Vision Graphics Image Process. 13 (1980) 257–269.
[38] B. Kosko, Neural Networks and Fuzzy Systems: A Dynamical Systems Approach to Machine Intelligence, Prentice-Hall, Englewood Cliffs, NJ, 1992.
[39] B. Kosko, Fuzzy cognitive maps, Int. J. Man Mach. Stud. 24 (1986) 65–75.
[40] S. Haykin, Neural Networks: A Comprehensive Foundation, Macmillan, New York, 1994.
[41] S.T. Barnard, Stochastic stereo matching over scale, Int. J. Comput. Vision 3 (1) (1989) 17–32.
[42] S. Hattori, A. Okamoto, H. Hasegawa, Stereo matching by simulated annealing incorporating a diffusion equation, Proceedings of the ASPRS 1998 Annual Conference, 1998, pp. 1030–1041.
[43] J.R. Hilera, V.J. Martínez, Redes Neuronales Artificiales, RA-MA, 1995.
[44] H.J. Zimmermann, Fuzzy Set Theory and its Applications, Kluwer Academic Publishers, Dordrecht, 1991.
[45] T. Poggio, V. Torre, C. Koch, Computational vision and regularization theory, Nature 317 (1985) 314–319.
[46] D.H. Ballard, Generalizing the Hough transform to detect arbitrary shapes, Pattern Recognition 13 (2) (1981) 111–122.
[47] S.B. Marapane, M.M. Trivedi, Region-based stereo analysis for robotic applications, IEEE Trans. Syst. Man Cybern. 19 (6) (1989) 1447–1464.
[48] A. Lopez, F. Pla, Dealing with segmentation errors in region-based stereo matching, Pattern Recognition 33 (2000) 1325–1338.